DESY 11–239
December 2011

ISSN 0418–9833

Associated production of Z and neutral Higgs bosons at the CERN Large Hadron Collider

Bernd A. Kniehl[1] and Caesar P. Palisoc[2]

[1] II. Institut für Theoretische Physik, Universität Hamburg,
Luruper Chaussee 149, 22761 Hamburg, Germany

[2] National Institute of Physics, University of the Philippines,
Diliman, Quezon City 1101, Philippines

Abstract

We study the hadroproduction of a CP-even or CP-odd neutral Higgs boson in association with a Z boson in the minimal supersymmetric extension of the standard model (MSSM) We include the contributions from quark-antiquark annihilation at the tree level and those from gluon-gluon fusion, which proceeds via quark and squark loops, and list compact analytic results. We quantitatively analyze the hadronic cross sections at the CERN Large Hadron Collider assuming a favorable supergravity-inspired MSSM scenario.

PACS numbers: 11.30.Pb, 12.60.Jv, 13.85.Qk, 14.80.Da

1 Introduction

The search for Higgs bosons is among the prime tasks of the CERN Large Hadron Collider (LHC) [1]. While the standard model (SM) of elementary-particle physics contains one complex Higgs doublet, from which one neutral CP-even Higgs boson H emerges in the physical particle spectrum after the spontaneous breakdown of the electroweak symmetry, the Higgs sector of the minimal supersymmetric extension of the SM (MSSM) consists of a two-Higgs-doublet model (2HDM) and accommodates a quintet of physical Higgs bosons: the neutral CP-even h^0 and H^0 bosons, the neutral CP-odd A^0 boson, and the charged $H^\pm$-boson pair. At the tree level, the MSSM Higgs sector has two free parameters, which are usually taken to be the mass m_{A^0} of the A^0 boson and the ratio $\tan\beta = v_2/v_1$ of the vacuum expectation values of the two Higgs doublets.

In the following, we focus our attention on the h^0 ,H^0, and A^0 bosons, which we collectively denote by ϕ. A recent discussion of $H^\pm$-boson production at the LHC may be found in Refs. [2–4] and the references cited therein. The dominant source of ϕ bosons is their single production by gg fusion, $gg \to \phi$, which is mediated by heavy-quark [5] and squark [6] loops. Another, less important mechanism of single ϕ-boson production is $b\bar{b} \to \phi$ [7]. The ϕ bosons thus produced have essentially zero transverse momentum (p_T). In order for the ϕ bosons to obtain finite p_T, they need to be produced in association with one or more other particles or jets (j). In leading order (LO), $j\phi$ associated production proceeds through the partonic subprocesses $gg \to g\phi$, $gq \to q\phi$, and $q\bar{q} \to g\phi$, which again involve heavy-quark [8,9] and squark [9,10] loops. Alternatively, the ϕ bosons can be produced, with interesting rates, in association with (i) a dijet via intermediate-boson fusion, $qq' \to qq'V^*V^* \to qq'\phi$, where q and q' stand for any light flavor of quark or antiquark, $V = W^\pm, Z$, and virtual particles are marked by an asterisk [11]; (ii) a quark-antiquark pair of heavy flavor $Q = t, b$ via $gg, q\bar{q} \to Q\bar{Q}\phi$ [12]; (iii) an intermediate boson via $q\bar{q}' \to W^\pm\phi$ [13–16], $q\bar{q} \to Z\phi$ [13,14,16–21], and $gg \to Z\phi$ [17–19,22–25]; or (iv) another, possibly different ϕ boson via $q\bar{q} \to \phi_1\phi_2$ [16,26,27] and $gg \to \phi_1\phi_2$ [27–29]. Note that, due to the absence of A^0VV couplings at the tree level, $qq' \to qq'V^*V^* \to qq'\phi$ and the Drell-Yan processes $q\bar{q}' \to W^{\pm *} \to W^\pm\phi$ and $q\bar{q} \to Z^* \to Z\phi$ are not possible for $\phi = A^0$. The partonic suprocesses $gg \to Z\phi$ and $gg \to \phi_1\phi_2$ are mediated by heavy-quark [17–19,22–25,27–29] and squark loops [18,27,29]. Comprehensive reviews of quantum corrections to Higgs-boson production within the SM and MSSM may be found in Refs. [30,31], respectively.

In this paper, we revisit $Z\phi$ associated hadroproduction via gluon fusion in the MSSM. In the SM case, mutual agreement between three independent calculations [17,22,25] has been established, and compact formulae for the partonic cross section are available [17]. In the MSSM, the status is much less advanced and, perhaps, somewhat unsatisfactory. As for $gg \to Z\phi$ with $\phi = h^0, H^0$, there exists only one analysis so far [19], which has not yet been verified by other authors. The analytic expressions presented in Ref. [19] are rather complicated; they involve 14 form factors. In order to translate the SM results [17,22,25] to the case of $gg \to Z\phi$ with $\phi = h^0, H^0$ in the MSSM, it is not sufficient to adjust the HZZ and Hqq couplings; it is also necessary to include certain quark triangle

diagrams with an A^0 boson in the s channel [see Fig. 1(a)]. On the other hand, the squark loop contributions to these two MSSM processes vanish [19] for reasons explained below. As for $gg \to ZA^0$, the quark loop contributions were first studied on the basis of a numerical evaluation [23], which was recently employed for phenomenological signal-versus-background analyses taking into account the subsequent $Z \to l^+l^-$ and $A^0 \to b\bar{b}$ decays [20,24]. An independent analysis, including also the squark loops, was reported in Ref. [18], which does not contain an analytic expression for the partonic cross section either. Unfortunately, comparisons between Refs. [18,20,23,24] are not discussed in these papers. Recently, the helicity amplitudes of $gg \to Z\phi$ with $\phi = h^0, H^0, A^0$ were analyzed in Ref. [32] with regard to the asymptotic helicity conservation property of supersymmetry, and their real and imaginary parts were graphically presented at a specific scattering angle as functions of the center-of-mass (c.m.) energy.

With the Higgs hunt at the LHC being in full swing, it is an urgent matter to consolidate our knowledge of $Z\phi$ associated hadroproduction via gluon fusion in the MSSM, which is the motivation of this paper. Specifically, we present compact analytic expressions, also for the partonic cross sections of $q\bar{q}, b\bar{b} \to Z\phi$ [18–21], and perform a detailed numerical analysis using up-to-date input.

The importance of $b\bar{b}$-initiated subprocesses for Higgs-boson production has been variously emphasized in the literature, in particular, in connection with the final states ϕ [7], $\phi_1\phi_2$ [27], H^+H^- [33], and $W^\pm H^\mp$ [2,34]. These subprocesses receive contributions from Feynman diagrams involving b-quark Yukawa couplings, which are generally strong for large values of $\tan\beta$. (The $\bar{b}tH^-$ and $\bar{t}bH^+$ couplings are also strong for small values of $\tan\beta$.) If the two final-state particles couple to a Z boson (or photon), as is the case for the final states h^0A^0, H^0A^0, Zh^0, ZH^0, and H^+H^-, then there are additional contributions from Drell-Yan-type diagrams, which are already present for the light flavors $q = u, d, s, c$. However, diagrams of the latter type are absent for the final states h^0h^0, h^0H^0, H^0H^0, A^0A^0, ZA^0, and $W^\pm H^\mp$, which can still be produced through $b\bar{b}$ annihilation.

As for $b\bar{b}$ annihilation, it should be noted that the treatment of bottom as an active flavor inside the colliding hadrons leads to an effective description, which comprises contributions from the higher-order subprocesses $gb \to Z\phi b$, $g\bar{b} \to Z\phi\bar{b}$, and $gg \to Z\phi b\bar{b}$. If all these subprocesses are to be explicitly included along with $b\bar{b} \to Z\phi$, then it is necessary to employ a judiciously subtracted b-quark PDF in order to avoid double counting [7,35]. The evaluation of $b\bar{b} \to Z\phi$ with an unsubtracted b-quark PDF is expected to slightly overestimate the true cross section [7,35]. For simplicity, we shall nevertheless adopt this effective approach in our analysis, keeping in mind that a QCD-correction factor below unity is to be applied. In fact, such a behavior has recently been observed for $b\bar{b} \to ZA^0$ [21].

In order to reduce the number of unknown supersymmetric input parameters, we adopt a scenario where the MSSM is embedded in a grand unified theory (GUT) involving supergravity (SUGRA) [36]. The MSSM thus constrained is characterized by the following parameters at the GUT scale, which come in addition to $\tan\beta$ and m_{A^0}: the universal scalar mass m_0, the universal gaugino mass $m_{1/2}$, the trilinear Higgs-sfermion coupling A, the bilinear Higgs coupling B, and the Higgs-higgsino mass parameter μ. Notice that m_{A^0}

is then not an independent parameter anymore, but it is fixed through the renormalization group equation. The number of parameters can be further reduced by making additional assumptions. Unification of the τ-lepton and b-quark Yukawa couplings at the GUT scale leads to a correlation between m_t and $\tan\beta$. Furthermore, if the electroweak symmetry is broken radiatively, then B and μ are determined up to the sign of μ. Finally, it turns out that the MSSM parameters are nearly independent of the value of A, as long as $|A| \lesssim 500$ GeV at the GUT scale.

This paper is organized as follows. In Sec. 2, we list the LO cross sections of $q\bar{q} \to Z\phi$, including the Yukawa-enhanced contributions for $q = b$, and those of $gg \to Z\phi$, including both quark and squark loop contributions, in the MSSM. The relevant quark and squark loop form factors are relegated to Appendix B. In Sec. 3, we present quantitative predictions for the inclusive cross sections of $pp \to Z\phi + X$ at the LHC adopting a favorable SUGRA-inspired MSSM scenario. Sec. 4 contains our conclusions. For the reader's convenience, the relevant Feynman rules are summarized in Appendix A.

2 Analytic Results

In this section, we present the LO cross sections of the partonic subprocesses $q\bar{q} \to Z\phi$ and $gg \to Z\phi$, where $\phi = h^0, H^0, A^0$, in the MSSM. We work in the parton model of QCD with $n_f = 5$ active quark flavors $q = u, d, s, c, b$, which we take to be massless. However, we retain the b-quark Yukawa couplings at their finite values, in order not to suppress possibly sizable contributions. We adopt the MSSM Feynman rules from Ref. [37]. The couplings of the Z and ϕ bosons to quarks, v_{Zqq}, a_{Zqq}, and $g_{\phi qq}$, are given in Eq. (5) of Ref. [33] and Eq. (A3) of Ref. [27], respectively. As for the ϕZZ couplings, g_{h^0ZZ} and g_{H^0ZZ} are given by Eq. (A.3) in Appendix A, while the A^0ZZ coupling vanishes at tree level. The h^0A^0Z and H^0A^0Z couplings, $g_{h^0A^0Z}$ and $g_{H^0A^0Z}$, may be found in Eq. (A2) of Ref. [27]. For each quark flavor q there is a corresponding squark flavor $\tilde{q}$, which comes in two mass eigenstates $i = 1, 2$. The masses $m_{\tilde{q}_i}$ of the squarks and their trilinear couplings to the ϕ bosons, $g_{\phi\tilde{q}_i\tilde{q}_j}$, are listed in Eqs. (A.5), (A.7), and (A.8) and in Table 1 of Ref. [38][1], Eq. (A.2) of Ref. [33], and Eq. (A4) of Ref. [27], respectively.

Considering the generic partonic subprocess $ab \to Z\phi$, we denote the four-momenta of the incoming partons, a and b, and the outgoing Z and ϕ bosons by p_a, p_b, p_Z, and p_ϕ, respectively, and define the partonic Mandelstam variables as $s = (p_a+p_b)^2$, $t = (p_a-p_Z)^2$, and $u = (p_b - p_Z)^2$. The on-shell conditions read $p_a^2 = p_b^2 = 0$, $p_Z^2 = m_Z^2 = z$, and $p_\phi^2 = m_\phi^2 = h$. Four-momentum conservation implies that $s+t+u = z+h$. Furthermore, we have $sp_T^2 = tu - zh = N$, where p_T is the absolute value of transverse momentum common to the Z and ϕ bosons in the c.m. frame.

The tree-level diagrams for $b\bar{b} \to Z\phi$ with $\phi = h^0, H^0$ and $\phi = A^0$ are depicted in Fig. 1(a) and (b), respectively. As already mentioned above, there is no Drell-Yan diagram in Fig. 1(b) because of the absence of a A^0ZZ coupling at the tree level. The differential cross sections for the first class of partonic subprocesses may be generically

[1] In Ref. [38], $m_{\tilde{q}_i}$ and $g_{\phi\tilde{q}_i\tilde{q}_j}$ are called $M_{\tilde{Q}a}$ and $\tilde{V}^{\phi}_{Qab}/g$, respectively.

written as

$$\frac{d\sigma}{dt}\left(b\bar{b}\to Z\phi\right)=\frac{G_F^2c_w^4z}{3\pi s}\left[\left(2z+p_T^2\right)g_{\phi ZZ}^2\left(v_{Zbb}^2+a_{Zbb}^2\right)|\mathcal{P}_Z(s)|^2+\lambda|P|^2\right.$$
$$\left.-\,4sp_T^2\left(\frac{1}{t}+\frac{1}{u}\right)g_{\phi bb}a_{Zbb}\,\mathrm{Re}\,P+g_{\phi bb}^2\left(v_{Zbb}^2T_++a_{Zbb}^2T_-\right)\right],\qquad(1)$$

where G_F is Fermi's constant, $c_w=m_W/m_Z$ is the cosine of the weak mixing angle, $\lambda=s^2+z^2+h^2-2(sz+zh+hs)$, and

$$P=g_{\phi A^0Z}g_{A^0bb}\mathcal{P}_{A^0}(s),$$
$$T_\pm=2\pm2+2p_T^2\left[z\left(\frac{1}{t}\pm\frac{1}{u}\right)\mp\frac{2s}{tu}\right].\qquad(2)$$

Here,

$$\mathcal{P}_X(s)=\frac{1}{s-m_X^2+im_X\Gamma_X}\qquad(3)$$

is the propagator function of particle X, with mass m_X and total decay width Γ_X. For the second class of partonic subprocesses, we have

$$\frac{d\sigma}{dt}\left(b\bar{b}\to ZA^0\right)=\frac{G_F^2c_w^4z}{3\pi s}\left[\lambda|S|^2-4sp_T^2\left(\frac{1}{t}+\frac{1}{u}\right)g_{A^0bb}a_{Zbb}\,\mathrm{Re}\,S\right.$$
$$\left.+\,g_{A^0bb}^2\left(v_{Zbb}^2T_++a_{Zbb}^2T_-\right)\right],\qquad(4)$$

where

$$S=g_{h^0A^0Z}g_{h^0bb}\mathcal{P}_{h^0}(s)+g_{H^0A^0Z}g_{H^0bb}\mathcal{P}_{H^0}(s).\qquad(5)$$

As for Zh^0 and ZH^0 production, there are also sizable contributions from $q\bar{q}$ annihilation via a virtual Z boson for the quarks of the first and second generations, $q=u,d,s,c$, whose Yukawa couplings are negligibly small. The corresponding Drell-Yan cross sections are obtained from Eq. (1) by putting $P=T_\pm=0$ and substituting $b\to q$. The resulting expression agrees with Eq. (2.8) of Ref. [17], appropriate for $q\bar{q}\to ZH$ in the SM, after adjusting the HZZ coupling. The full tree-level cross sections are then obtained by complementing the $b\bar{b}$-initiated cross sections of Eq. (1) with the Drell-Yan cross sections for $q=u,d,s,c$.

The non-vanishing one-loop diagrams pertinent to $gg\to Z\phi$, with $\phi=h^0,H^0$ and $\phi=A^0$ are depicted in Figs. 2(a) and (b), respectively. As already mentioned in the Introduction, the presence of the quark triangle diagrams involving an s-channel A^0-boson exchange in Fig. 2(a) represents a qualitatively new feature of the MSSM as compared to the SM. Furthermore, similarly to Fig. 1(b), quark triangle diagrams with an s-channel Z-boson exchange do not appear in Fig. 2(b). In the following, we refer to a squark loop diagram involving an s-channel propagator as a triangle diagram. The residual squark loop diagrams are regarded to be of box type. The squark triangle and box diagrams for $gg\to Z\phi$ with $\phi=h^0,H^0$ vanish, and so do the squark box diagrams for $gg\to ZA^0$. This may be understood as follows. (i) The $g_{g\tilde{q}_i\tilde{q}_j}$, $g_{gg\tilde{q}_i\tilde{q}_j}$, $g_{gZ\tilde{q}_i\tilde{q}_j}$, and $g_{Z\tilde{q}_i\tilde{q}_j}$ couplings

are symmetric in i and j, while the $g_{A^0\tilde{q}_i\tilde{q}_j}$ coupling is antisymmetric [39]. Thus, squark loops connecting gluons and Z bosons with an odd number of A^0 bosons vanish upon summation over i and j. (ii) The $g_{g\tilde{q}_i\tilde{q}_j}$ and $g_{Z\tilde{q}_i\tilde{q}_j}$ couplings are linear in the squark four-momenta, while the $g_{gg\tilde{q}_i\tilde{q}_j}$, $g_{gZ\tilde{q}_i\tilde{q}_j}$, and $g_{\phi\tilde{q}_i\tilde{q}_j}$ couplings are momentum independent [39]. Thus, a squark loop connecting gluons, Z bosons, and ϕ bosons vanishes upon adding its counterpart with the loop-momentum flows reversed if the total number of gluons and Z bosons is odd.

As in Refs. [3,4], we express the quark and squark loop contributions in terms of helicity amplitudes. We label the helicity states of the two gluons and the Z boson in the partonic c.m. frame by $\lambda_a = \pm 1/2$, $\lambda_b = \pm 1/2$, and $\lambda_Z = 0, \pm 1$. We first consider $gg \to Z\phi$ with $\phi = h^0, H^0$. The helicity amplitudes of the quark triangle contribution read

$$\begin{aligned}\mathcal{M}^{\triangle}_{\lambda_a\lambda_b 0} = -2\sqrt{\frac{\lambda}{z}}(\lambda_a + \lambda_b)\sum_q \Bigg[\frac{z-s}{z}\, a_{Zqq} g_{\phi ZZ} \mathcal{P}_Z(s)\left(F_{\triangle}\left(s, m_q^2\right) + 2\right) \\ - \frac{s}{m_q} g_{A^0qq} g_{\phi A^0 Z} \mathcal{P}_{A^0}(s) F_{\triangle}\left(s, m_q^2\right)\Bigg]. \end{aligned} \tag{6}$$

The quark triangle form factor, $F_{\triangle}$, is given in Eq. (B.7). As for the quark box contribution, all twelve helicity combinations contribute. Due to Bose symmetry, they are related by

$$\begin{aligned}\mathcal{M}^{\square}_{\lambda_a\lambda_b\lambda_Z}(t,u) &= (-1)^{\lambda_Z}\mathcal{M}^{\square}_{\lambda_b\lambda_a\lambda_Z}(u,t), \\ \mathcal{M}^{\square}_{\lambda_a\lambda_b\lambda_Z}(t,u) &= \mathcal{M}^{\square}_{-\lambda_a-\lambda_b-\lambda_Z}(t,u). \end{aligned} \tag{7}$$

Keeping $\lambda_Z = \pm 1$ generic, we thus only need to specify four expressions. These read

$$\begin{aligned}\mathcal{M}^{\square}_{++0} &= \frac{8}{\sqrt{z\lambda}}\sum_q g_{\phi qq} a_{Zqq} m_q \left[F^0_{++} + (t \leftrightarrow u)\right], \\ \mathcal{M}^{\square}_{+-0} &= \frac{8}{\sqrt{z\lambda}}\sum_q g_{\phi qq} a_{Zqq} m_q \left[F^0_{+-} - (t \leftrightarrow u)\right], \\ \mathcal{M}^{\square}_{++\lambda_Z} &= -4\sqrt{\frac{2N}{s}}\sum_q g_{\phi qq} a_{Zqq} m_q \left[F^1_{++} - (t \leftrightarrow u)\right], \\ \mathcal{M}^{\square}_{+-\lambda_Z} &= -4\sqrt{\frac{2N}{s}}\sum_q g_{\phi qq} a_{Zqq} m_q \left[F^1_{+-} + (t \leftrightarrow u, \lambda_Z \leftrightarrow -\lambda_Z)\right]. \end{aligned} \tag{8}$$

The quark box form factors, $F^{|\lambda_Z|}_{\lambda_a\lambda_b}$, are listed in Eq. (B.8). For the reasons explained above, we have $\tilde{\mathcal{M}}^{\triangle}_{\lambda_a\lambda_b\lambda_Z} = \tilde{\mathcal{M}}^{\square}_{\lambda_a\lambda_b\lambda_Z} = 0$ for the squark-induced helicity amplitudes.

We now turn to $gg \to ZA^0$. The helicity amplitudes of the quark and squark triangle contributions read

$$\mathcal{M}^{\triangle}_{\lambda_a\lambda_b 0} = -8\sqrt{\frac{\lambda}{z}}(1 + \lambda_a\lambda_b)\sum_q m_q \left(g_{h^0A^0Z} g_{h^0qq}\mathcal{P}_{h^0}(s) + g_{H^0A^0Z} g_{H^0qq}\mathcal{P}_{H^0}(s)\right) F_{\triangle}\left(s, m_q^2\right),$$

(9)

$$\tilde{\mathcal{M}}^{\triangle}_{\lambda_a\lambda_b 0} = 2\sqrt{\frac{\lambda}{z}}(1+\lambda_a\lambda_b)\sum_{\tilde{q}_i}\left(g_{h^0A^0Z}g_{h^0\tilde{q}_i\tilde{q}_i}\mathcal{P}_{h^0}(s) + g_{H^0A^0Z}g_{H^0\tilde{q}_i\tilde{q}_i}\mathcal{P}_{H^0}(s)\right)\tilde{F}_{\triangle}\left(s, m^2_{\tilde{q}_i}\right), \tag{10}$$

respectively. The quark and squark triangle form factors, $F_{\triangle}$ and $\tilde{F}_{\triangle}$, may be found in Eq. (B.9). Again, the helicity amplitudes of the quark box contribution satisfy the Bose symmetry relations of Eq. (7). We find

$$\begin{aligned}
\mathcal{M}^{\square}_{++0} &= -\frac{8}{\sqrt{z\lambda}}\sum_q g_{A^0qq}a_{Zqq}m_q\left[F^0_{++} + (t\leftrightarrow u)\right],\\
\mathcal{M}^{\square}_{+-0} &= -\frac{8}{\sqrt{z\lambda}}\sum_q g_{A^0qq}a_{Zqq}m_q\left[F^0_{+-} + (t\leftrightarrow u)\right],\\
\mathcal{M}^{\square}_{++\lambda_Z} &= -4\sqrt{\frac{2N}{s}}\sum_q g_{A^0qq}a_{Zqq}m_q\left[F^1_{++} - (t\leftrightarrow u)\right],\\
\mathcal{M}^{\square}_{+-\lambda_Z} &= -4\sqrt{\frac{2N}{s}}\sum_q g_{A^0qq}a_{Zqq}m_q\left[F^1_{+-} - (t\leftrightarrow u, \lambda_Z\to-\lambda_Z)\right].
\end{aligned} \tag{11}$$

The quark box form factors, $F^{|\lambda_Z|}_{\lambda_a\lambda_b}$, are presented in Eq. (B.10). We recall that $\tilde{\mathcal{M}}^{\square}_{\lambda_a\lambda_b\lambda_Z} = 0$.

The differential cross section of $gg\to Z\phi$ is then given by

$$\frac{d\sigma}{dt}(gg\to Z\phi) = \frac{\alpha_s^2(\mu_r)G_F^2m_W^4}{256(4\pi)^3s^2}\sum_{\lambda_a,\lambda_b,\lambda_Z}\left|\mathcal{M}^{\triangle}_{\lambda_a\lambda_b\lambda_Z} + \mathcal{M}^{\square}_{\lambda_a\lambda_b\lambda_Z} + \tilde{\mathcal{M}}^{\triangle}_{\lambda_a\lambda_b\lambda_Z}\right|^2, \tag{12}$$

where $\alpha_s(\mu_r)$ is the strong-coupling constant at renormalization scale μ_r. Due to Bose symmetry, the right-hand side of Eq. (12) is symmetric in t and u.

The differential cross section of $gg\to ZH$ in the SM is obtained from Eqs. (6)–(8) and (12), with $\phi = h^0$, by replacing $h^0\to H$, adjusting the h^0ZZ and h^0qq couplings, and discarding the contribution due to A^0-boson exchange. In this way, we recover the result of Ref. [17], which is expressed in terms of Lorentz-invariant form factors rather than helicity amplitudes.

The kinematics of the inclusive reaction $AB\to Z\phi + X$, where A and B are colliding hadrons, is described in Sec. II of Ref. [2]. Its double-differential cross section $d^2\sigma/dy\,dp_T$, where y and p_T are the rapidity and transverse momentum of the Z boson in the c.m. system of the hadronic collision, may be evaluated from Eq. (2.1) of Ref. [2].

3 Phenomenological Implications

We are now in a position to explore the phenomenological implications of our results. The SM input parameters for our numerical analysis are taken to be $G_F = 1.16637\times$

10^{-5} GeV^{-2}, $m_W = 80.399$ GeV, $m_Z = 91.1876$ GeV, $m_t = 172.0$ GeV , and $\overline{m}_b(\overline{m}_b) = 4.19$ GeV [40]. We adopt the LO proton PDF set CTEQ6L1 [41]. We evaluate $\alpha_s(\mu_r)$ and $m_b(\mu_r)$ from the LO formulas, which may be found, *e.g.*, in Eqs. (23) and (24) of Ref. [42], respectively, with $n_f = 5$ quark flavors and asymptotic scale parameter $\Lambda^{(5)}_{\rm QCD} = 165$ MeV [41]. We identify the renormalization and factorization scales with the $Z\phi$ invariant mass $\sqrt{s}$. We vary $\tan\beta$ and m_{A^0} in the ranges $3 < \tan\beta < 32 \approx m_t/m_b$ and 180 GeV $< m_{A^0} <$ 1 TeV, respectively. As for the GUT parameters, we choose $m_{1/2} = 150$ GeV, $A = 0$, and $\mu < 0$, and tune m_0 so as to be consistent with the desired value of m_{A^0}. All other MSSM parameters are then determined according to the SUGRA-inspired scenario as implemented in the program package SUSPECT [43]. We do not impose the unification of the τ-lepton and b-quark Yukawa couplings at the GUT scale, which would just constrain the allowed $\tan\beta$ range without any visible effect on the results for these values of $\tan\beta$. We exclude solutions which do not comply with the present experimental lower mass bounds of the sfermions, charginos, neutralinos, and Higgs bosons [40].

We now study the fully integrated cross sections of $pp \to Z\phi + X$ at the LHC, with c.m. energy $\sqrt{S} = 14$ TeV. Figures 3–5 refer to the cases $\phi = h^0, H^0, A^0$, respectively. In part (a) of each figure, the m_ϕ dependence is studied for $\tan\beta = 3$ and 30 while, in part (b), the $\tan\beta$ dependence is studied for $m_{A^0} = 300$ and 600 GeV. We note that the SUGRA-inspired MSSM with our choice of input parameters does not permit $\tan\beta$ and m_{A^0} to be simultaneously small, due to the experimental lower bound on m_{h^0} [40]. This explains why the curves for $\tan\beta = 3$ in Figs. 3–5(a) only start at $m_{A^0} \approx 280$ GeV, while those for $\tan\beta = 30$ already start at $m_{A^0} \approx 180$ GeV.

In Figs. 3 and 4, which refer to $\phi = h^0, H^0$, respectively, the total $q\bar{q}$-annihilation contributions (dashed lines), corresponding to the coherent superposition of Drell-Yan and Yukawa-enhanced amplitudes, and the gg-fusion contributions (solid lines), which arise only from quark loops, are presented separately. For a comparison with future experimental data, they should be added. For comparison, also the pure Drell-Yan contributions (dotted lines) are shown. As for $\phi = h^0$, we observe from Fig. 3 that the contribution due to $q\bar{q}$ annihilation is almost exhausted by the Drell-Yan process and greatly exceeds the one due to gg fusion, by a factor of 3–5. The $q\bar{q}$-annihilation contribution falls off by a factor of two as m_{h^0} runs from 82 GeV to 115 GeV and feebly depends on $\tan\beta$, except for the appreciable rise towards the lower edge of the considered $\tan\beta$ range. The gg-fusion contribution feebly depends on m_{h^0}, m_{A^0}, and $\tan\beta$. The situation is very different for $\phi = H^0$, as is obvious from Fig. 4. Here, $b\bar{b}$ annihilation is generally far more important than the Drell-Yan process, except for $m_{A^0} = 300$ GeV and $\tan\beta = 3$, where the latter gets close. The contribution due to $b\bar{b}$ annihilation monotonically increases with $\tan\beta$, while the one due to the Drell-Yan process decreases. Furthermore, gg fusion competes with $q\bar{q}$ annihilation and even dominates for $\tan\beta \lesssim 7$.

As for $\phi = A^0$, the $b\bar{b}$-annihilation contribution (dashed lines) and the total gg-fusion contribution (solid lines), corresponding to the coherent superposition of quark and squark loop amplitudes, are presented separately in Fig. 5. For comparison, also the gg-fusion contribution due to quark loops only (dotted lines) is shown. As in the case of $\phi = H^0$,

gg fusion competes with $b\bar{b}$ annihilation and even dominates for $\tan\beta \lesssim 7$. Again, the $b\bar{b}$-annihilation contribution monotonically increases with $\tan\beta$. The bulk of the gg-fusion contribution is due to the quark loops, especially at low values of m_{A^0}.

Finally, we compare our results with the literature. As already mentioned in Sec. 2, we recover the well-known SM result [17], for $\phi = H$, by taking the SM limit of our results for $\phi = h^0$ in Eqs. (6) and (8). The contribution due to A^0-boson exchange in Eq. (6), which is not probed in the SM limit, agrees with the analogous contribution to $gg \to W^-H^+$ given in Eq. (1) of Ref. [3] after appropriately adjusting the masses and couplings. On the other hand, the residual terms in the latter equation, which arise from the exchanges of h^0 and H^0 bosons, coincide with Eq. (9) after substituting the appropriate masses and couplings. Similarly, by adjusting masses and couplings in Eq. (10), we reproduce Eq. (2.3) in Ref. [4], which gives the squark triangle contribution to $gg \to W^-H^+$. In Ref. [23], numerical results for the cross section of $pp \to ZA^0$ via quark-loop-mediated gg fusion were presented. Adopting the input parameters and proton PDF set specified in that reference, we nicely reproduce the separate contributions due triangle and box diagrams shown in Fig. 4 therein, while we fail to agree with their superposition. Furthermore, we find reasonable agreement with the cross section of $pp \to ZA^0 + X$ via gg fusion represented graphically for different scenarios in Figs. 6 and 7 of Ref. [21] adopting the respective inputs from there.

4 Conclusions

We analytically calculated the cross sections of the partonic subprocesses $q\bar{q} \to Z\phi$ and $gg \to Z\phi$, where $\phi = h^0, H^0, A^0$, to LO in the MSSM. We included the Drell-Yan and Yukawa-enhanced contributions to $q\bar{q}$ annihilation (see Fig. 1) and the quark and squark loop contributions to gg fusion (see Fig. 2). We presented these results as helicity amplitudes expressed in terms of standard scalar one-loop integrals.

We then quantitatively investigated the inclusive cross sections of $pp \to Z\phi + X$ at the LHC with $\sqrt{S} = 14$ GeV adopting a favorable SUGRA-inspired MSSM scenario, varying the input parameters m_{A^0} and $\tan\beta$. Our results are presented in Figs. 3–5. The total cross section for $\phi = h^0$ is typically of order 1 pb, while those for $\phi = H^0, A^0$ are of order 100 fb (10 fb) for $m_{A^0} = 300$ GeV (600 GeV). Assuming design luminosity, $L = 10^{34}$ cm^{-2}s^{-1}, a cross section of 1 pb corresponds to 10^5 events per year and experiment at the LHC (see Table I of Ref. [44]).

Acknowledgments

We thank A. A. Barrientos Bendezu and R. Ziegler for their collaboration at the initial stage of this work. The work of B.A.K. was supported in part by the German Federal Ministry for Education and Research BMBF through Grant No. 05 HT6GUA, by the German Research Foundation DFG through the Collaborative Research Centre No. 676 *Particles, Strings and the Early Universe—The Structure of Matter and Space Time*, and

by the Helmholtz Association HGF through the Helmholtz Alliance Ha 101 *Physics at the Terascale*. The work of C.P.P. was supported in part by the German Academic Exchange Service (DAAD) Reinvitation Programme under Reference Code A/07/02820 and by the Office of the Vice President for Academic Affairs of the University of the Philippines.

A Feynman rules

In this appendix, we collect the Feynman rules used in this paper. The Feynman rules for the $Zq\overline{q}$ vertices are $ig\gamma^\mu(v_{Zqq} - a_{Zqq}\gamma_5)$, with $g = e/s_w$, e being the proton charge, $s_w^2 = 1 - c_w^2$, and

$$v_{Zqq} = -\frac{I_q - 2s_w^2 Q_q}{2c_w}, \qquad a_{Zqq} = -\frac{I_q}{2c_w}, \tag{A.1}$$

where $I_q = \pm 1/2$ and $Q_q = 2/3, -1/3$ are the weak hypercharge and electric charge of quark q, respectively. The Feynman rules for the $\phi q\overline{q}$ ($\phi = h^0, H^0$) and $A^0 q\overline{q}$ vertices are $igg_{\phi qq}$ and $gg_{A^0qq}\gamma_5$, respectively, with

$$\begin{aligned}
g_{h^0tt} &= -\frac{m_t \cos\alpha}{2m_W \sin\beta}, \qquad & g_{H^0tt} &= -\frac{m_t \sin\alpha}{2m_W \sin\beta}, \qquad & g_{A^0tt} &= -\frac{m_t \cot\beta}{2m_W}, \\
g_{h^0bb} &= \frac{m_b \sin\alpha}{2m_W \cos\beta}, \qquad & g_{H^0bb} &= -\frac{m_b \cos\alpha}{2m_W \cos\beta}, \qquad & g_{A^0bb} &= -\frac{m_b \tan\beta}{2m_W},
\end{aligned} \tag{A.2}$$

where α is the mixing angle that rotates the weak CP-even Higgs eigenstates into the mass eigenstates h^0 and H^0. The Feynman rules for the ϕZZ vertices are $igg_{\phi ZZ}g^{\mu\nu}$, with

$$g_{h^0ZZ} = -\frac{m_Z}{c_w}\sin(\alpha - \beta), \qquad g_{H^0ZZ} = \frac{m_Z}{c_w}\cos(\alpha - \beta). \tag{A.3}$$

The Feynman rules for the $\phi A^0 Z$ vertices are $gg_{\phi A^0 Z}(p + p')^\mu$, where p is the incoming four-momentum of the ϕ boson, p' is the outgoing four-momentum of the A^0 boson, and

$$g_{h^0A^0Z} = \frac{\cos(\alpha - \beta)}{2c_w}, \qquad g_{H^0A^0Z} = \frac{\sin(\alpha - \beta)}{2c_w}. \tag{A.4}$$

The Feynman rules for the $\phi\tilde{q}_i\tilde{q}_j$ vertices are $igg_{\phi\tilde{q}_i\tilde{q}_j}$, with

$$\begin{aligned}
&\begin{pmatrix} g_{h^0\tilde{t}_1\tilde{t}_1} & g_{h^0\tilde{t}_1\tilde{t}_2} \\ g_{h^0\tilde{t}_2\tilde{t}_1} & g_{h^0\tilde{t}_2\tilde{t}_2} \end{pmatrix} \\
&= \mathcal{M}^{\tilde{t}} \begin{pmatrix} \frac{m_Z \sin(\alpha+\beta)\left(I_t^3 - s_w^2 Q_t\right)}{c_w} - \frac{m_t^2 \cos\alpha}{m_W \sin\beta} & -\frac{m_t(\mu \sin\alpha + A_t \cos\alpha)}{2m_W \sin\beta} \\ -\frac{m_t(\mu \sin\alpha + A_t \cos\alpha)}{2m_W \sin\beta} & \frac{m_Z \sin(\alpha+\beta) s_w^2 Q_t}{c_w} - \frac{m_t^2 \cos\alpha}{m_W \sin\beta} \end{pmatrix} \left(\mathcal{M}^{\tilde{t}}\right)^T, \\
&\begin{pmatrix} g_{h^0\tilde{b}_1\tilde{b}_1} & g_{h^0\tilde{b}_1\tilde{b}_2} \\ g_{h^0\tilde{b}_2\tilde{b}_1} & g_{h^0\tilde{b}_2\tilde{b}_2} \end{pmatrix} \\
&= \mathcal{M}^{\tilde{b}} \begin{pmatrix} \frac{m_Z \sin(\alpha+\beta)\left(I_b^3 - s_w^2 Q_b\right)}{c_w} + \frac{m_b^2 \sin\alpha}{m_W \cos\beta} & \frac{m_b(\mu \cos\alpha + A_b \sin\alpha)}{2m_W \cos\beta} \\ \frac{m_b(\mu \cos\alpha + A_b \sin\alpha)}{2m_W \cos\beta} & \frac{m_Z \sin(\alpha+\beta) s_w^2 Q_b}{c_w} + \frac{m_b^2 \sin\alpha}{m_W \cos\beta} \end{pmatrix} \left(\mathcal{M}^{\tilde{b}}\right)^T,
\end{aligned}$$

$$
\begin{aligned}
&\begin{pmatrix} g_{H^0\tilde{t}_1\tilde{t}_1} & g_{H^0\tilde{t}_1\tilde{t}_2} \\ g_{H^0\tilde{t}_2\tilde{t}_1} & g_{H^0\tilde{t}_2\tilde{t}_2} \end{pmatrix} \\
&= \mathcal{M}^{\tilde{t}} \begin{pmatrix} -\frac{m_Z \cos(\alpha+\beta)\left(I_t^3 - s_w^2 Q_t\right)}{c_w} - \frac{m_t^2 \sin\alpha}{m_W \sin\beta} & \frac{m_t(\mu\cos\alpha - A_t \sin\alpha)}{2 m_W \sin\beta} \\ \frac{m_t(\mu\cos\alpha - A_t\sin\alpha)}{2 m_W \sin\beta} & -\frac{m_Z \cos(\alpha+\beta) s_w^2 Q_t}{c_w} - \frac{m_t^2 \sin\alpha}{m_W \sin\beta} \end{pmatrix} \left(\mathcal{M}^{\tilde{t}}\right)^T, \\
&\begin{pmatrix} g_{H^0\tilde{b}_1\tilde{b}_1} & g_{H^0\tilde{b}_1\tilde{b}_2} \\ g_{H^0\tilde{b}_2\tilde{b}_1} & g_{H^0\tilde{b}_2\tilde{b}_2} \end{pmatrix} \\
&= \mathcal{M}^{\tilde{b}} \begin{pmatrix} -\frac{m_Z \cos(\alpha+\beta)\left(I_b^3 - s_w^2 Q_b\right)}{c_w} - \frac{m_b^2 \cos\alpha}{m_W \cos\beta} & \frac{m_b(\mu\sin\alpha - A_b \cos\alpha)}{2 m_W \cos\beta} \\ \frac{m_b(\mu\sin\alpha - A_b\cos\alpha)}{2 m_W \cos\beta} & -\frac{m_Z \cos(\alpha+\beta) s_w^2 Q_b}{c_w} - \frac{m_b^2 \cos\alpha}{m_W \cos\beta} \end{pmatrix} \left(\mathcal{M}^{\tilde{b}}\right)^T, \quad \text{(A.5)}
\end{aligned}
$$

where

$$
\mathcal{M}^{\tilde{q}} = \begin{pmatrix} \cos\theta_{\tilde{q}} & \sin\theta_{\tilde{q}} \\ -\sin\theta_{\tilde{q}} & \cos\theta_{\tilde{q}} \end{pmatrix} \quad \text{(A.6)}
$$

are the squark mixing matrices, with $\theta_{\tilde{q}}$ being the squark mixing angles.

B Quark and squark loop form factors

In this appendix, we express the quark and squark triangle and box form factors, $F_\triangle$, $\tilde{F}_\triangle$, and $F^{|\lambda_Z|}_{\lambda_a\lambda_b}$, for $\phi = h^0, H^0$ and $\phi = A^0$, in terms of the standard scalar three- and four-point functions, which we abbreviate as $C^{ab}_{ijk}(c) = C_0\left(a,b,c,m_i^2,m_j^2,m_k^2\right)$ and $D^{abcd}_{ijkl}(e,f) = D_0\left(a,b,c,d,e,f,m_i^2,m_j^2,m_k^2,m_l^2\right)$, respectively. The definitions of the latter may be found in Eq. (5) of Ref. [3].

The quark triangle form factor for $\phi = h^0, H^0$ reads

$$
F_\triangle\left(s, m_q^2\right) = 4 m_q^2 C^{00}_{qqq}(s). \quad \text{(B.7)}
$$

The quark box form factors for $\phi = h^0, H^0$ read

$$
\begin{aligned}
F^0_{++} &= 2s(t+u)C^{00}_{qqq}(s) + 2\left(t+u+\frac{\lambda}{s}\right)\left[(t-z)C^{z0}_{qqq}(t) + (t-h)C^{h0}_{qqq}(t)\right] \\
&\quad - \left[N\left(t+u+\frac{\lambda}{s}\right) + 2m_q^2\lambda\right] D^{h0z0}_{qqqq}(t,u) - 4\left(szh + m_q^2\lambda\right) D^{hz00}_{qqqq}(s,t), \\
F^0_{+-} &= \frac{(h-z-s)}{N}(t-u)\left[s(t+u)C^{00}_{qqq}(s) - \lambda C^{hz}_{qqq}(s) - 2m_q^2 N D^{h0z0}_{qqqq}(t,u)\right] \\
&\quad + 2(t+u)(t-z)\left[1 + \frac{t(t-u)(h-z-s)}{N(t+u)}\right] C^{z0}_{qqq}(t) \\
&\quad + \frac{2(t-h)}{N}\left[z(u^2-t^2-\lambda) + (t+u)(t^2-zh)\right] C^{h0}_{qqq}(t) \\
&\quad - (h-z-s)\left[2st\frac{t^2-zh}{N} + 4m_q^2(t-u)\right] D^{hz00}_{qqqq}(s,t),
\end{aligned}
$$

$$
\begin{aligned}
F^1_{++} &= (t-u)\left[\frac{z-h-s}{\sqrt{\lambda}}-\lambda_Z\right]\left[\frac{s}{N}C^{00}_{qqq}(s)-\frac{1}{2}D^{h0z0}_{qqqq}(t,u)-\frac{s}{N}\left(t+\frac{2N}{t-u}\right)D^{hz00}_{qqqq}(s,t)\right]\\
&\quad+\frac{2(h-u)}{\sqrt{\lambda}N}\left(\lambda_Z\sqrt{\lambda}+t-u+\frac{2N}{h-u}\right)\left[(h-t)C^{h0}_{qqq}(t)+(z-u)C^{z0}_{qqq}(u)\right],\\
F^1_{+-} &= \frac{s}{N}\left(\frac{4s(t+u)}{\sqrt{\lambda}}+\sqrt{\lambda}-\lambda_Z(t-u)\right)C^{00}_{qqq}(s)-\frac{2s}{N}\left(\sqrt{\lambda}+\lambda_Z(t-u)\right)C^{hz}_{qqq}(s)\\
&\quad-\frac{2(t-h)}{\sqrt{\lambda}N}\left(-s(u+3t)-2N+(u-t)(t-z)+\lambda_Z(t-s-z)\sqrt{\lambda}\right)C^{h0}_{qqq}(t)\\
&\quad+\frac{2(u-z)}{\sqrt{\lambda}N}\left(3u(s-z)+th-2z(h-2u)-\lambda_Z(h-u)\sqrt{\lambda}\right)C^{z0}_{qqq}(u)\\
&\quad+\frac{s}{\sqrt{\lambda}N}\left[t\left(\lambda+8zh-4ts-2(t+u)(z+h)\right.\right.\\
&\quad+\left.\left.\lambda_Z(-2h+3t+u-2z)\sqrt{\lambda}\right)-16m_q^2N\right]D^{hz00}_{qqqq}(s,t)\\
&\quad+\frac{1}{2}\left(-\sqrt{\lambda}-\frac{16m_q^2s}{\sqrt{\lambda}}+\lambda_Z(t-u)\right)D^{h0z0}_{qqqq}(t,u).
\end{aligned}
\tag{B.8}
$$

The quark and squark triangle form factors for $\phi = A^0$ read

$$
\begin{aligned}
F_\triangle\left(s,m_q^2\right) &= 2+\left(4m_q^2-s\right)C^{00}_{qqq}(s),\\
\tilde{F}_\triangle\left(s,m_{\tilde{q}}^2\right) &= 2+4m_{\tilde{q}_i}^2C^{00}_{\tilde{q}_i\tilde{q}_i\tilde{q}_i}(s).
\end{aligned}
\tag{B.9}
$$

The quark box form factors for $\phi = A^0$ read

$$
\begin{aligned}
F^0_{++} &= 2s(t+u)C^{00}_{qqq}(s)+2\left(t+u+\frac{\lambda}{s}\right)\left[(t-z)C^{z0}_{qqq}(t)+(t-h)C^{h0}_{qqq}(t)\right]\\
&\quad-\left[N\left(t+u+\frac{\lambda}{s}\right)+2m_q^2\lambda\right]D^{h0z0}_{qqqq}(t,u)-4\left(szh+m_q^2\lambda\right)D^{hz00}_{qqqq}(s,t),\\
F^0_{+-} &= -\left[2+\frac{(t-u)^2}{N}\right]\left[s(t+u)C^{00}_{qqq}(s)-\lambda C^{hz}_{qqq}(s)\right]\\
&\quad-2\left[3t-u+\frac{t}{N}(t-u)^2\right]\left[(t-z)C^{z0}_{qqq}(t)+(t-h)C^{h0}_{qqq}(t)\right]\\
&\quad-2\left(zN-m_q^2\lambda\right)D^{h0z0}_{qqqq}(t,u)\\
&\quad+2\left\{st\left[3t-u+\frac{t}{N}(t-u)^2\right]+2m_q^2\lambda\right\}D^{hz00}_{qqqq}(s,t),\\
F^1_{++} &= \left(\frac{z-h-s}{\sqrt{\lambda}}-\lambda_Z\right)\left\{(t-u)\left(\frac{s}{N}C^{00}_{qqq}(s)-\frac{1}{2}D^{h0z0}_{qqqq}(t,u)\right)\right.\\
&\quad-\left.s\left[2+\frac{t}{N}(t-u)\right]D^{hz00}_{qqqq}(s,t)\right\}\\
&\quad+2(t-z)\left\{\lambda_Z\frac{h-t}{N}+\frac{1}{\sqrt{\lambda}}\left[2+\frac{(t-u)(t-h)}{N}\right]\right\}C^{z0}_{qqq}(t)
\end{aligned}
$$

$$
\begin{aligned}
&- 2(t-h)\left\{\lambda_Z\frac{h-u}{N}+\frac{1}{\sqrt{\lambda}}\left[2-\frac{(t-u)(u-h)}{N}\right]\right\}C^{h0}_{qqq}(t),\\
F^1_{+-} = &\left(\lambda_Z-\frac{t-u}{\sqrt{\lambda}}\right)\left[\frac{s}{N}(s-z+h)\left(C^{00}_{qqq}(s)-tD^{hz00}_{qqqq}(s,t)\right)+\frac{s+z-h}{2}D^{h0z0}_{qqqq}(t,u)\right]\\
&- 2(t-z)\left\{\lambda_Z\frac{t-h}{N}-\frac{1}{\sqrt{\lambda}}\left[2+\frac{(t-u)(t-h)}{N}\right]\right\}C^{z0}_{qqq}(t)\\
&- 2(t-h)\left\{\lambda_Z\frac{u-h}{N}+\frac{1}{\sqrt{\lambda}}\left[2-\frac{(t-u)(u-h)}{N}\right]\right\}C^{h0}_{qqq}(t). \qquad \text{(B.10)}
\end{aligned}
$$

References

[1] Z. Kunszt and F. Zwirner, Nucl. Phys. B **385**, 3 (1992) [arXiv:hep-ph/9203223], and references cited therein.

[2] A. A. Barrientos Bendezu and B. A. Kniehl, Phys. Rev. D **59**, 015009 (1999) [arXiv:hep-ph/9807480].

[3] A. A. Barrientos Bendezu and B. A. Kniehl, Phys. Rev. D **61**, 097701 (2000) [arXiv:hep-ph/9909502].

[4] A. A. Barrientos Bendezu and B. A. Kniehl, Phys. Rev. D **63**, 015009 (2001) [arXiv:hep-ph/0007336].

[5] H. M. Georgi, S. L. Glashow, M. E. Machacek, and D. V. Nanopoulos, Phys. Rev. Lett. **40**, 692 (1978).

[6] S. Dawson, A. Djouadi, and M. Spira, Phys. Rev. Lett. **77**, 16 (1996) [arXiv:hep-ph/9603423].

[7] D. A. Dicus and S. Willenbrock, Phys. Rev. D **39**, 751 (1989); D. Dicus, T. Stelzer, Z. Sullivan, and S. Willenbrock, *ibid.* **59**, 094016 (1999) [arXiv:hep-ph/9811492].

[8] R. K. Ellis, I. Hinchliffe, M. Soldate, and J. J. van der Bij, Nucl. Phys. **B297**, 221 (1988); U. Baur and E. W. N. Glover, *ibid.* **B339**, 38 (1990); U. Langenegger, M. Spira, A. Starodumov, and P. Trüb, JHEP **0606**, 035 (2006) [arXiv:hep-ph/0604156].

[9] O. Brein and W. Hollik, Phys. Rev. D **68**, 095006 (2003) [arXiv:hep-ph/0305321]; **76**, 035002 (2007) [arXiv:0705.2744 [hep-ph]].

[10] M. Mühlleitner and M. Spira, Nucl. Phys. **B790**, 1 (2008) [arXiv:hep-ph/0612254].

[11] R. N. Cahn and S. Dawson, Phys. Lett. **136B**, 196 (1984); **138B**, 464(E) (1984).

[12] Z. Kunszt, Nucl. Phys. **B247**, 339 (1984).

[13] S. L. Glashow, D. V. Nanopoulos, and A. Yildiz, Phys. Rev. D **18**, 1724 (1978); E. Eichten, I. Hinchliffe, K. D. Lane, and C. Quigg, Rev. Mod. Phys. **56**, 579 (1984); **58**, 1065(E) (1986); Z. Kunszt, Z. Trocsanyi, and W. J. Stirling, Phys. Lett. B **271**, 247 (1991).

[14] T. Han and S. Willenbrock, Phys. Lett. B **273**, 167 (1991).

[15] J. Ohnemus and W. J. Stirling, Phys. Rev. D **47**, 2722 (1993); H. Baer, B. Bailey, and J. F. Owens, *ibid.* **47**, 2730 (1993).

[16] A. Djouadi and M. Spira, Phys. Rev. D **62**, 014004 (2000) [arXiv:hep-ph/9912476].

[17] B. A. Kniehl, Phys. Rev. D **42**, 2253 (1990); Phys. Lett. B **244**, 537 (1990); Phys. Rev. D **42**, 3100 (1990).

[18] J. Yin, W.-G. Ma, R.-Y. Zhang and, H.-S. Hou, Phys. Rev. D **66**, 095008 (2002).

[19] L. L. Yang, C. S. Li, J. J. Liu and L. G. Jin, J. Phys. G: Nucl. Part. Phys. **30**, 1821 (2004) [arXiv:hep-ph/0312179].

[20] C. Kao and S. Sachithanandam, Phys. Lett. B **620**, 80 (2005) [arXiv:hep-ph/0411331].

[21] Q. Li, C. S. Li, J. J. Liu, L. G. Jin and C. P. Yuan, Phys. Rev. D **72**, 034032 (2005) [arXiv:hep-ph/0501070].

[22] D. A. Dicus and C. Kao, Phys. Rev. D **38**, 1008 (1988); **42**, 2412(E) (1990).

[23] C. Kao, Phys. Rev. D **46**, 4907 (1992).

[24] C. Kao, G. Lovelace, and L. H. Orr, Phys. Lett. B **567**, 259 (2003) [arXiv:hep-ph/0305028].

[25] O. Brein, A. Djouadi, and R. Harlander, Phys. Lett. B **579**, 149 (2004) [arXiv:hep-ph/0307206].

[26] S. Dawson, S. Dittmaier, and M. Spira, Phys. Rev. D **58**, 115012 (1998) [arXiv:hep-ph/9805244].

[27] A. A. Barrientos Bendezu and B. A. Kniehl, Phys. Rev. D **64**, 035006 (2001) [arXiv:hep-ph/0103018].

[28] T. Plehn, M. Spira, and P. M. Zerwas, Nucl. Phys. **B479**, 46 (1996); **B531**, 655(E) (1998) [arXiv:hep-ph/9603205].

[29] A. Belyaev, M. Drees, O. J. P. Eboli, J. K. Mizukoshi, and S. F. Novaes, Phys. Rev. D **60**, 075008 (1999) [arXiv:hep-ph/9905266].

[30] B. A. Kniehl, Phys. Rept. **240**, 211 (1994); A. Djouadi, Phys. Rept. **457**, 1 (2008). [arXiv:hep-ph/0503172].

[31] M. Spira, Fortsch. Phys. **46**, 203 (1998) [arXiv:hep-ph/9705337]; M.S. Carena and H.E. Haber, Prog. Part. Nucl. Phys. **50**, 63 (2003) [arXiv:hep-ph/0208209]; A. Djouadi, Phys. Rept. **459**, 1 (2008) [arXiv:hep-ph/0503173].

[32] G. J. Gounaris, J. Layssac, and F. M. Renard, Phys. Rev. D **80**, 013009 (2009) [arXiv:0903.4532 [hep-ph]].

[33] A. A. Barrientos Bendezu and B. A. Kniehl, Nucl. Phys. **B568**, 305 (2000) [arXiv:hep-ph/9908385].

[34] D. A. Dicus, J. L. Hewett, C. Kao, and T. G. Rizzo, Phys. Rev. D **40**, 787 (1989); D. A. Dicus and C. Kao, *ibid.* **41**, 832 (1990); O. Brein, W. Hollik, and S. Kanemura, *ibid.* **63**, 095001 (2001) [arXiv:hep-ph/0008308]; W. Hollik and S.-H. Zhu, *ibid.* **65**, 075015 (2002) [arXiv:hep-ph/0109103].

[35] J. F. Gunion, H. E. Haber, F. E. Paige, W.-K. Tung, and S. S. D. Willenbrock, Nucl. Phys. **B294**, 621 (1987); R. M. Barnett, H. E. Haber, and D. E. Soper, *ibid.* **B306**, 697 (1988); F. I. Olness and W.-K. Tung, *ibid.* **B308**, 813 (1988); V. Barger, R. J. N. Phillips, and D. P. Roy, Phys. Lett. B **324**, 236 (1994) [arXiv:hep-ph/9311372]; M. A. G. Aivazis, J. C. Collins, F. I. Olness, and W. K. Tung, Phys. Rev. D **50**, 3102 (1994) [arXiv:hep-ph/9312319]; J. C. Collins, *ibid.* **58**, 094002 (1998) [arXiv:hep-ph/9806259]; M. Krämer, F. I. Olness, and D. E. Soper, *ibid.* **62**, 096007 (2000) [arXiv:hep-ph/0003035].

[36] A. Djouadi, J. Kalinowski, P. Ohmann, and P. M. Zerwas, Z. Phys. C **74**, 93 (1997) [arXiv:hep-ph/9605339].

[37] H. E. Haber and G. L. Kane, Phys. Rept. **117**, 75 (1985); J. F. Gunion and H. E. Haber, Nucl. Phys. **B272**, 1 (1986); **B402**, 567(E) (1993); **B278**, 449 (1986); **B402**, 569(E) (1993); **B307**, 445 (1988); **B402**, 569(E) (1993); J. F. Gunion, H. E. Haber, G. Kane, and S. Dawson, *The Higgs Hunter's Guide* (Addison-Wesley, Redwood City, 1990).

[38] R. Hempfling and B. A. Kniehl, Z. Phys. C **59**, 263 (1993).

[39] J. Rosiek, Phys. Rev. D **41**, 3464 (1990).

[40] Particle Data Group, K. Nakamura *et al.*, J. Phys. G **37**, 075021 (2010).

[41] J. Pumplin, D. R. Stump, J. Huston, H.-L. Lai, P. Nadolsky, and W.-K. Tung, JHEP **0207**, 012 (2002) [arXiv:hep-ph/0201195].

[42] B. A. Kniehl, Z. Phys. C **72**, 437 (1996) [arXiv:hep-ph/9403386].

[43] A. Djouadi, J. L. Kneur, and G. Moultaka, Comput. Phys. Commun. **176**, 426 (2007) [arXiv:hep-ph/0211331].

[44] B. A. Kniehl, C. P. Palisoc, and L. Zwirner, Phys. Rev. D **66**, 114002 (2002) [arXiv:hep-ph/0208104].

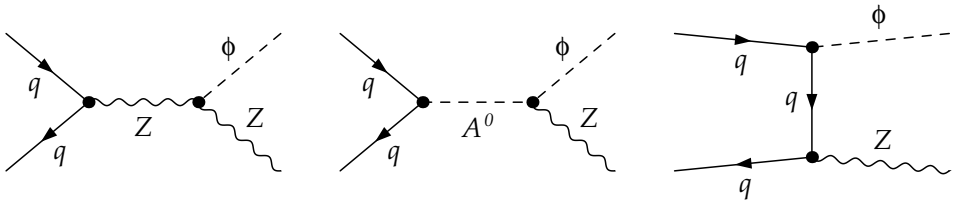

(a)

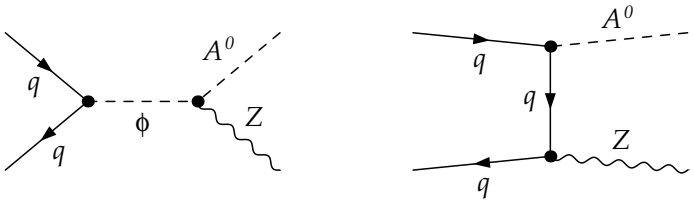

(b)

Figure 1: Tree-level Feynman diagrams for $q\bar{q} \to Z\phi$, with (a) $\phi = h^0, H^0$ and (b) $\phi = A^0$, in the MSSM.

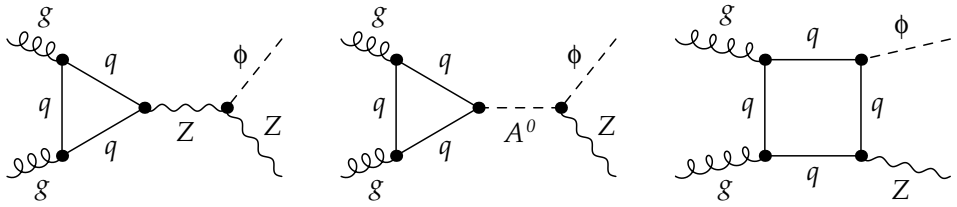

(a)

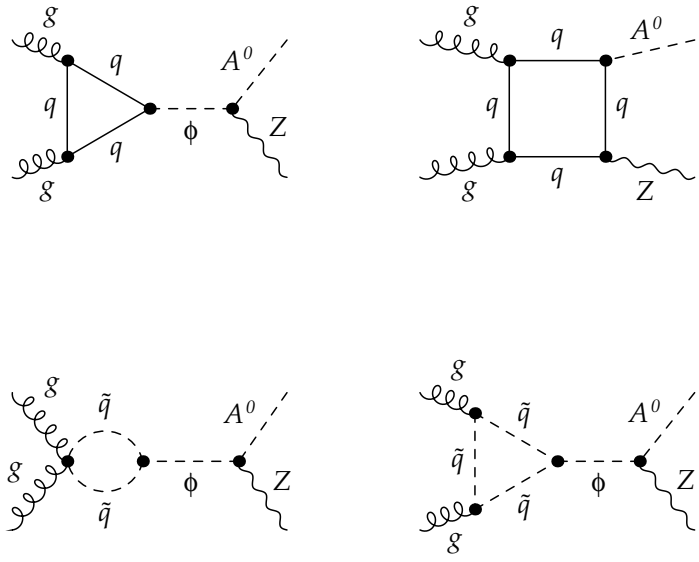

(b)

Figure 2: One-loop Feynman diagrams for $gg \to Z\phi$, with (a) $\phi = h^0, H^0$ and (b) $\phi = A^0$, due to virtual quarks and squarks in the MSSM.

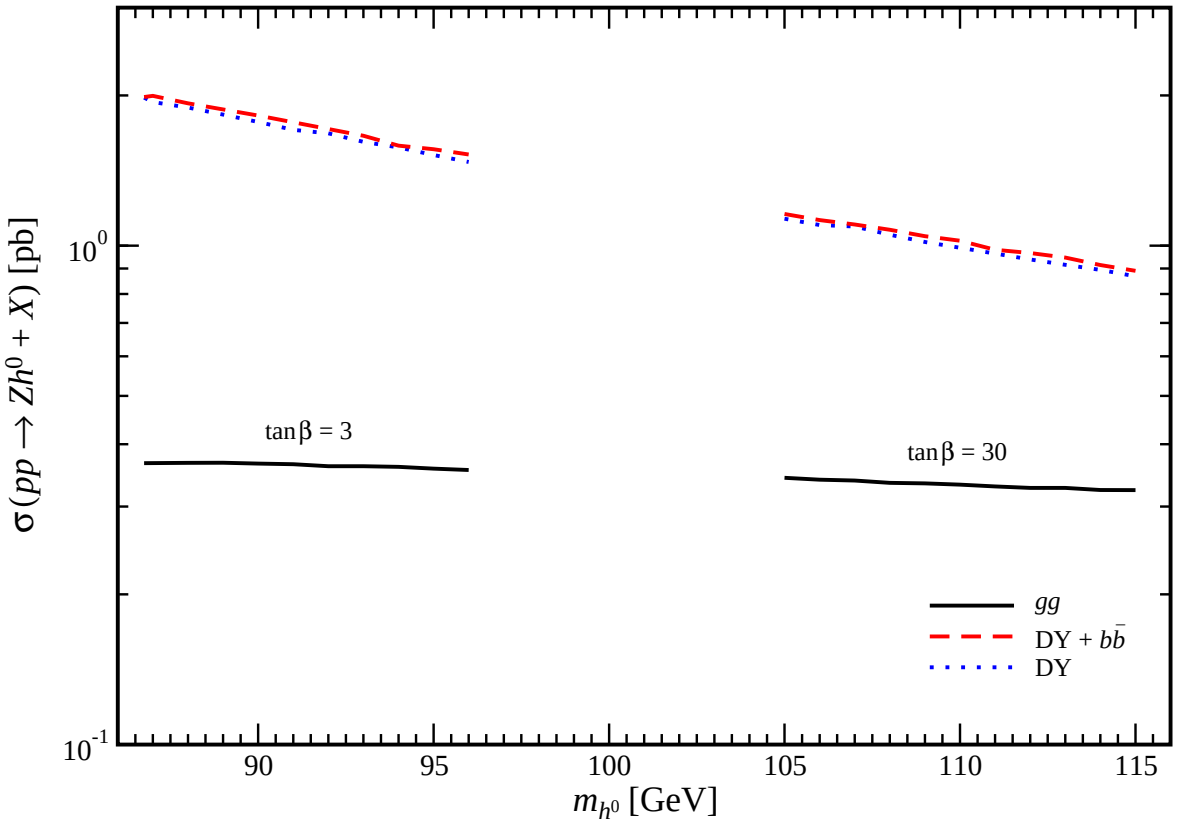

(a)

Figure 3: Total cross sections σ (in pb) of $pp \to Zh^0 + X$ via $q\bar{q}$ annihilation (dashed lines) and gg fusion (solid lines) at the LHC (a) as functions of m_{h^0} for $\tan\beta = 3$ and 30; and (b) as functions of $\tan\beta$ for $m_{A^0} = 300$ GeV and 600 GeV. For comparison, also the Drell-Yan contribution to $q\bar{q}$ annihilation (dotted lines) is shown.

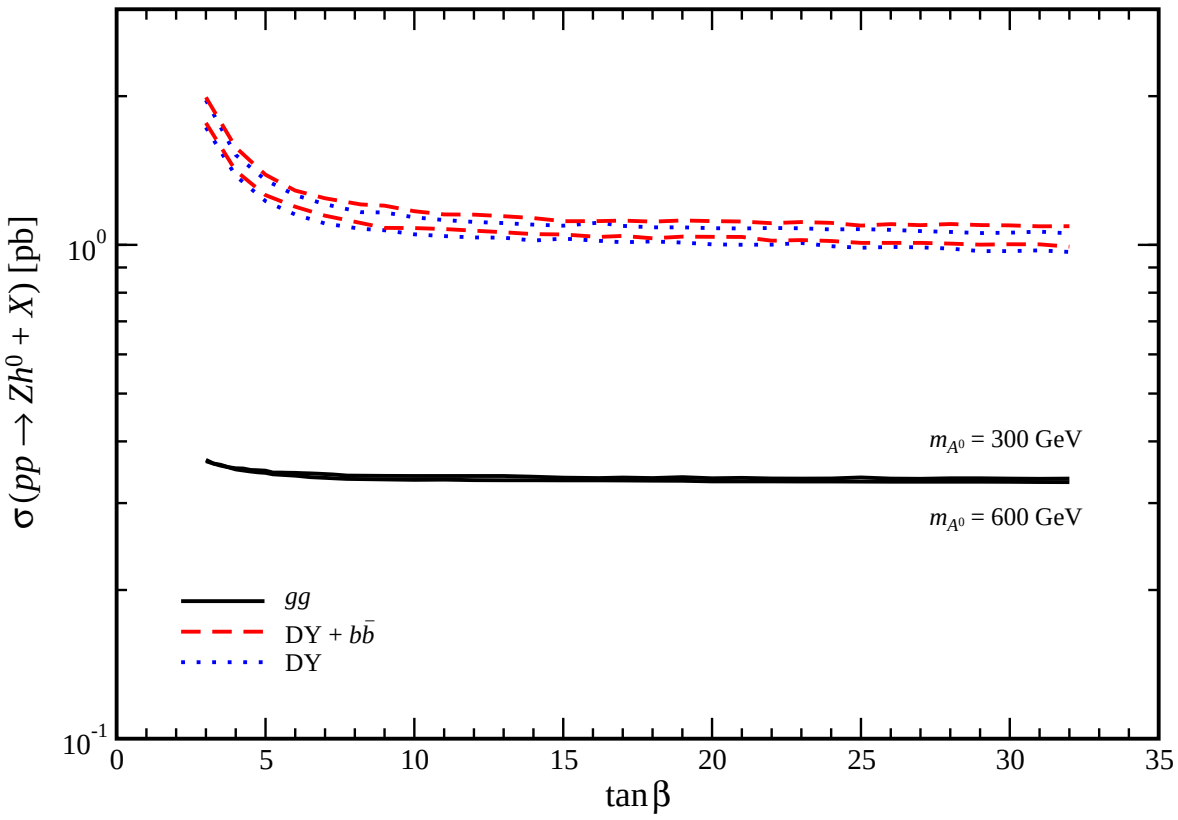

(b)

Figure 3 (Continued).

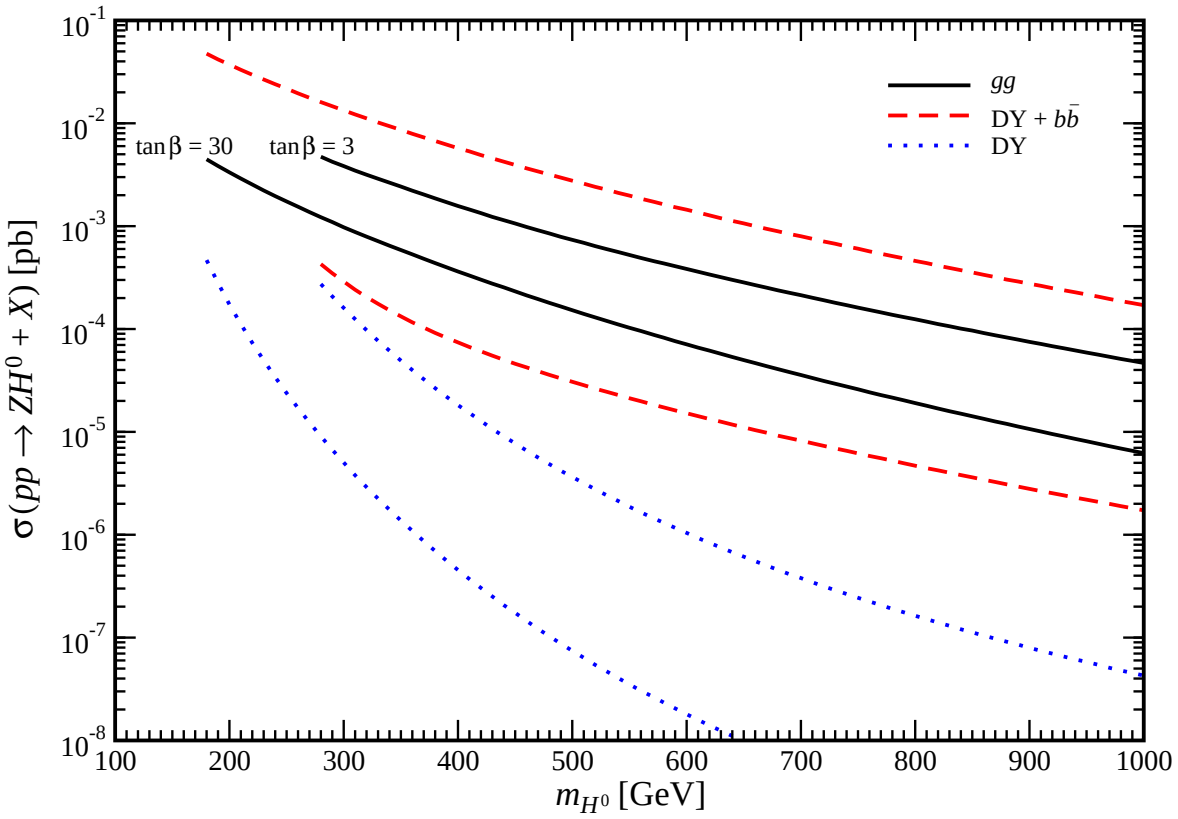

(a)

Figure 4: Total cross sections σ (in pb) of $pp \to ZH^0 + X$ via $q\bar{q}$ annihilation (dashed lines) and gg fusion (solid lines) at the LHC (a) as functions of m_{H^0} for $\tan\beta = 3$ and 30; and (b) as functions of $\tan\beta$ for $m_{A^0} = 300$ GeV and 600 GeV. For comparison, also the Drell-Yan contribution to $q\bar{q}$ annihilation (dotted lines) is shown.

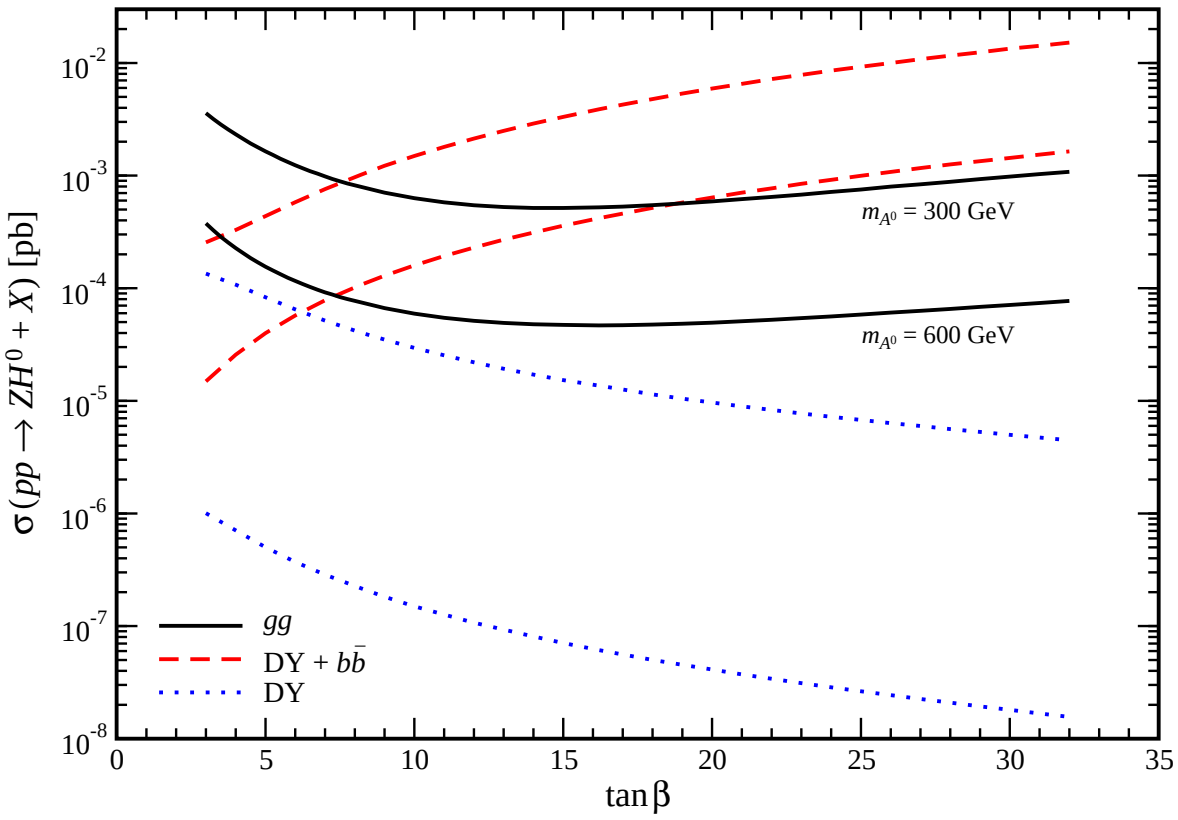

(b)

Figure 4 (Continued).

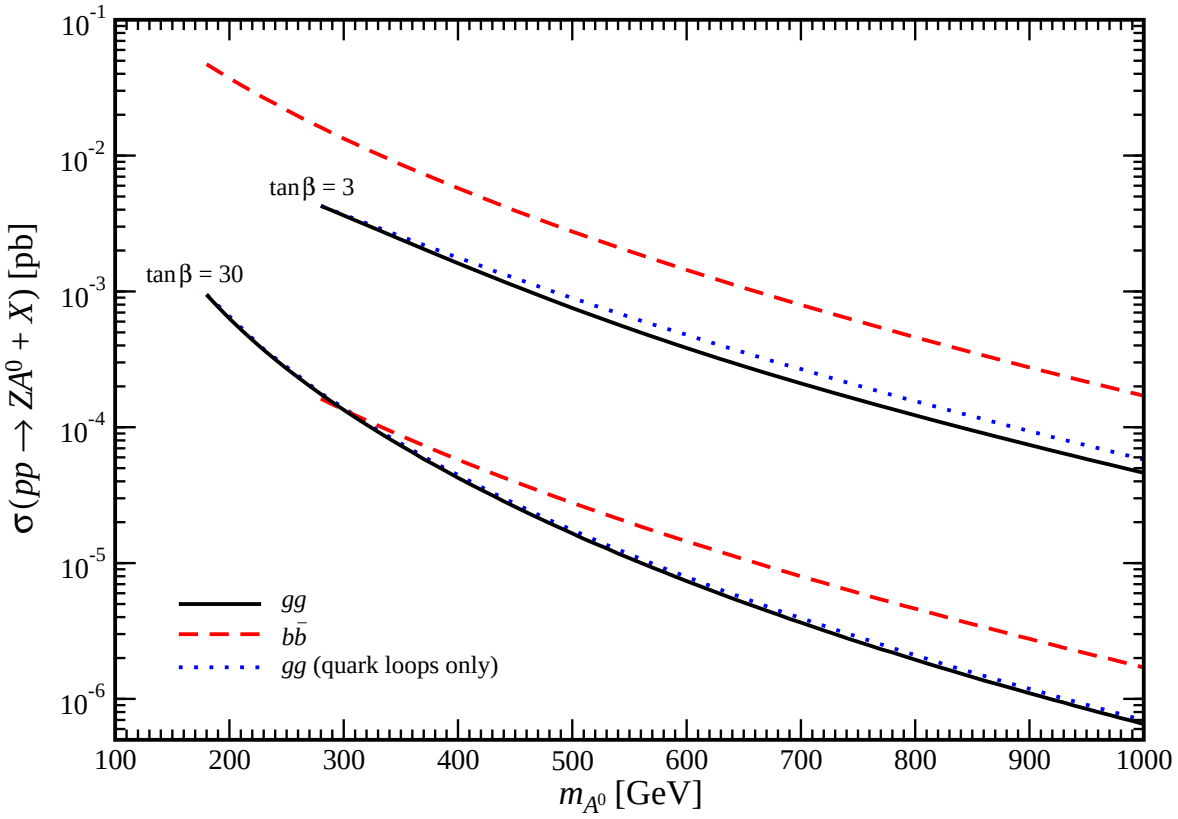

(a)

Figure 5: Total cross sections σ (in pb) of $pp \to ZA^0 + X$ via $b\bar{b}$ annihilation (dashed lines) and gg fusion (solid lines) at the LHC (a) as functions of m_{A^0} for $\tan\beta = 3$ and 30; and (b) as functions of $\tan\beta$ for $m_{A^0} = 300$ GeV and 600 GeV. For comparison, also the quark loop contribution to gg fusion (dotted lines) is shown.

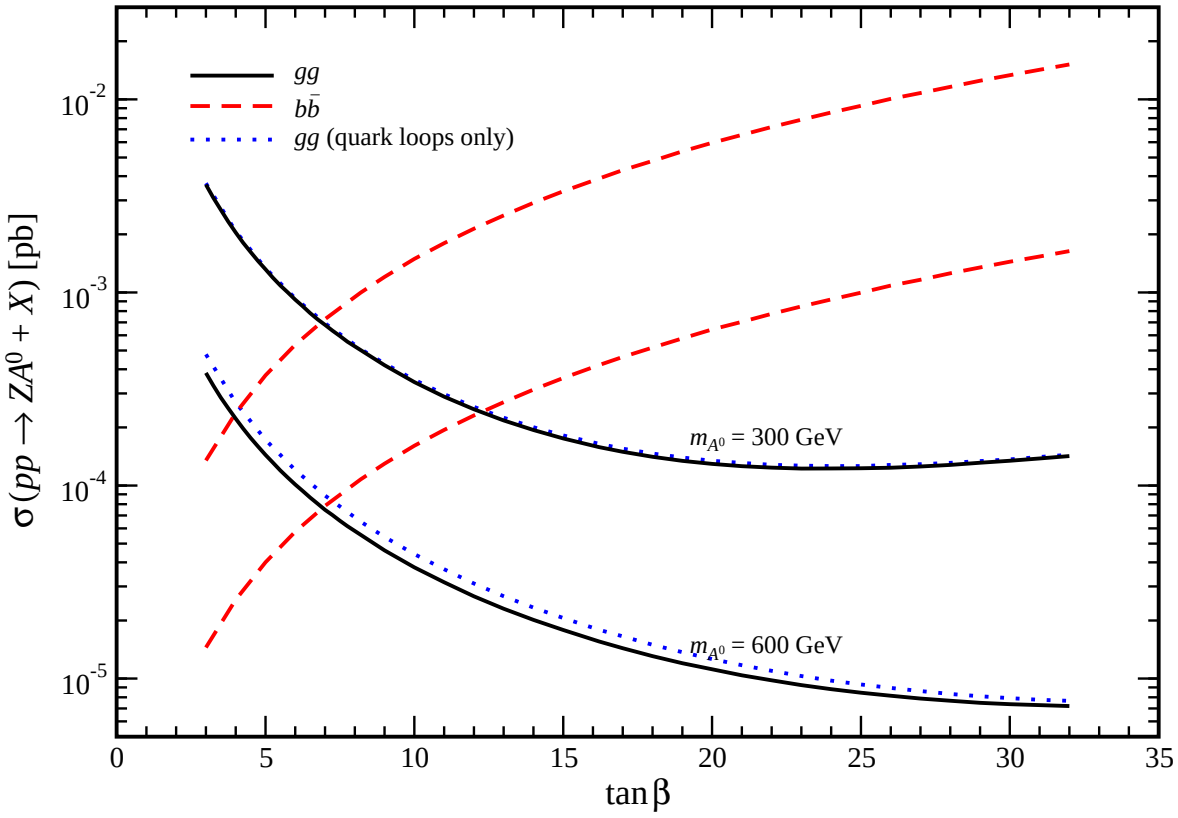

(b)

Figure 5 (Continued).